

Received: 2014.04.09
Accepted: 2014.04.22
Published: 2014.05.15

Anatomical study of suboccipital vertebral arteries and surrounding bony structures using virtual reality technology

Authors' Contribution:
Study Design A
Data Collection B
Statistical Analysis C
Data Interpretation D
Manuscript Preparation E
Literature Search F
Funds Collection G

EF 1 **Wenbo Ha***
BD 2 **DeLin Yang***
AG 2 **Shixin Gu**
DE 2 **Qi-Wu Xu**
BF 2 **Xiaoming Che**
DF 2 **Jin-Song Wu**
AG 3 **Wensheng Li**

1 Department of Neurosurgery, 5th Hospital affiliated Harbin Medical College, Daqing, China
2 Department of Neurosurgery, Huashun Hospital, Shanghai Medical College, Fudan University, Shanghai, China
3 Department of Anatomy, Shanghai Medicine Institute, Fudan University, Shanghai, China

* Wenbo Ha and DeLin Yang MD is co-first author

Corresponding Author: Shixin Gu, e-mail: gushixin@fudan.edu.cn
Source of support: Departmental sources

Background: This work aimed to evaluate the efficacy of virtual reality (VR) technology in neurosurgical anatomy through a comparison of the virtual 3D microanatomy of the suboccipital vertebral arteries and their bony structures as part of the resection of tumors in the craniovertebral junction (CVJ) of 20 patients compared to the actual microanatomy of the vertebral arteries of 15 cadaveric headsets.

Material/Methods: The study was conducted with 2 groups of data: a VR group composed of 20 clinical cases and a physical body group (PB group) composed of 15 cadaveric headsets. In the VR group, the dissection and measurements of the vertebral arteries were simulated on a Dextroscope. In the PB group, the vertebral arteries in the cadaver heads were examined under a microscope and anatomical measurements of VA and bony structures were performed. The length and course of the vertebral arteries and its surrounding bony structures in each group were compared.





Results: The distances from the inferior part of the transverse process foramen (TPF) of C1 to the inferior part of TPF of C2 were 17.68 ± 2.86 mm and 18.4 ± 1.82 mm in the PB and VR groups, respectively. The distances between the middle point of the posterior arch of the atlas and the medial intersection of VA on the groove were 17.35 ± 2.23 mm in the PB group and 18.13 ± 2.58 mm in the VR group. The distances between the middle line and the entrance of VA to the lower rim of TPF of Atlas were 28.64 ± 2.67 mm in PB group and 29.23 ± 2.89 mm in VR group. The diameters of the vertebral artery (VA) at the end of the groove and foramen of C2 transverse process were 4.02 ± 0.46 mm and 4.25 ± 0.51 mm, respectively, in the PB group and 3.54 ± 0.44 mm and 4.47 ± 0.62 mm, respectively, in VR group. The distances between the VA lumen center and midline of the foramen magnum at the level of dural penetration was 10.4 ± 1.13 mm in the PB group and 11.5 ± 1.34 mm in the VR group ($P > 0.05$).

Conclusions: VR technology can accurately simulate the anatomical features of the suboccipital vertebral arteries and their bony structures, which facilitates the planning of individual surgeries in the CVJ.

MeSH Keywords: **Cerebral Revascularization • Vertebral Artery • Virtual Reality Exposure Therapy**

Abbreviations: **CT** – computerized tomography; **MRI** – magnetic resonance imaging; **VR** – virtual reality; **CTA** – computerized tomography angiography; **MRA** – magnetic resonance angiography; **VA** – vertebral artery; **CVJ** – craniovertebral junction; **VHP** – Visible Human Project

Full-text PDF: <http://www.medscimonit.com/download/index/idArt/890840>

 1742  2  —  23

Background

The term *craniovertebral junction* (CVJ) refers to an area comprising the inferior portion of the occipital bone surrounding the foramen magnum and the first 2 cervical vertebrae. Knowledge on the bony configuration, vascular supply, and the courses of suboccipital vertebral arteries, as well as the kinetic anatomy of the craniocervical junction, is essential for successful skull base surgery. Owing to the variations and pathological anatomy alteration of suboccipital vertebral arteries (VAs), surgeries in the CVJ remain challenging for neurosurgeons [1].

Virtual reality (VR) is a multidisciplinary technology that has various uses and has also been applied to human body anatomical research such as in the case of the USA Visible Human Project (VHP), education in medicine [2–5], and clinical practice [6,7]. Although more anatomical studies of vertebral arteries have been conducted on topics such as corpus microsurgical anatomy or images [8–19], few individual anatomical studies on the occipital VAs have used the VR technique with a Dextroscope, especially those on the application of VA to CVJ surgery. We hypothesized that VR technology can demonstrate the individual anatomy of the occipital VAs and surrounding bony structure in 3D before CVJ tumor surgery.

Material and Methods

Groups

The study was performed on 2 groups of data: a Virtual Reality Group (VR Group) composed of 20 clinical cases with tumors that were confined to the CVJ, and a Physical Body Group (PB Group) that included 15 cadaveric headsets.

Twenty patients underwent imaging protocols with a 3D whole-body magnetic resonance imaging (MRI) scanner (General Electric Medical Systems, GE Signa VH/i) and a SOMATOM Sensation 64-slice computerized tomography (CT) scanner (Siemens AG). The imaging data were then loaded into the Dextroscope surgical planning workstation (Bracco Group, Milan, Italy) using RadioDexter software Version 1.0 R2, after which these data were processed.

The 15 cadaveric adult headset specimens were dissected using a microsurgical anatomy equipment set.

Dextroscope hardware and software

The Dextroscope is a surgical planning system that provides both 2D and 3D image processing environments. The 2D environment enables the loading of DICOM data using the standard mouse and keyboard approach. In a 3D environment, the Dextroscope

creates a stereoscopic 3D virtual workspace in which the user works with both hands to manipulate the patient-specific multimodal 3D imaging data using various image processing and surgical planning tools. A natural 3D user interface is created by reflecting the computer-generated 3D scenario by a mirror into the user's eyes. Wearing liquid-display shutter glasses synchronized with the time-split display, the user reaches with both hands behind the mirror into the "floating" 3D data.

The Dextroscope provides the tools necessary for 3D data exploration and surgical planning. By touching the physical bottom base of the workspace inside the Dextroscope with a handheld pen, a "virtual tool rack" automatically appears. This tool provides access to virtual buttons and sliders and can be activated with the virtual pen instrument [7]. Software tools are available for color and transparency coding; manual and semi-automatic segmentation; image fusion; curved, linear, and volumetric measurements; cropping and cutting in any angle; virtual tissue removal (virtual "drilling" or "suctioning") and reconstruction; as well as photograph and video reporting tools [7].

Image data acquisition

The scanning of patients was scheduled 1–3 days before surgery, and the imaging data were transferred to a Dextroscope in the laboratory by using a CD-ROM. MRI studies were performed on a GE 3.0 Tesla Signal Horizon Magnetic Resonance Scanner using Neuronavigation mode with the following imaging parameters: T₁WI FSPGR for the General Electric unit, TR/TE=9/2 ms; flip angle=25°; slice thickness=2 mm; interval=0; matrix size=256×256; field of view (FOV)=240×240 mm; and horizontal scanning range from the second cervical vertebra body to the cranial top. Gadopentetate dimeglumine was intravenously injected into the enhancement films. Magnetic resonance angiography (MRA) was performed in 3D time-of-flight mode and set with the following parameters: slice thickness=1.5 mm; interval=0; FOV=240×240 mm; and matrix size=256×256. Computerized tomography angiography (CTA) was performed on the 256-slice CT scanner following the intravenous contrast agent injection. CTA images were obtained contiguously as axial 1-mm slices (FOV=240×240 mm; matrix size=256×256) with horizontal scanning range from the third cervical vertebra body to the cranial top.

VR anatomy and topical anatomy

In the Dextroscope, co-registration was performed between the cranium, segmented from the head CTA or magnetic resonance angiography (MRA) and the MRI. The virtual anatomical dissections of the vertebral arteries and bony skull base were accomplished through the segmentation of the MRA or CTA of the head on the Dextroscope workstation for all the clinical patients. This process involved the measurement of

Table 1. Length and diameter of suboccipital VAs.

Group	PB group	VR group
No. of sides	30	40
Dis. bet. inf. part of C1TPF & inf. part of C2TPF (mm)	18.4±1.82	17.68±2.86
Dist. bet. middle point of posterior arch of atlas & medial intersection of VA on groove (mm)	17.35±2.23	18.13±2.58
Dist. bet. middle line & the entrance of VA to the lower rim of TPF of atlas (mm)	28.64±2.67	29.23±2.89
The diameter of VA at C2TPF (mm)	4.25±0.51	4.47±0.62
The diameter of VA at the ending of VA groove (mm)	4.02±0.46	3.54±0.44
Dist. bet. VA lumen center & midline of FM	10.4±1.13	11.5±1.34

Dist. – distance; bet. – between; inf. – inferior; C1 – atlas; TPF – transverse process foramen; C2 – axis; VA – vertebral artery.

the length and diameters of each part of suboccipital VAs in CVJ and the distance between bony structures, as well as the data on occipital condyle and magnum foramen.

Actual anatomical dissections of the VAs and measurement of bony structures were performed on the corresponding cadaveric specimens.

Statistical analysis

SPSS12.0 software was used in this stage. The paired t-test was used to examine quantitative data and RIDIT analysis was used to process numerical data. A P value less than 0.05 denotes a significant difference in the test.

Results

Courses and measurement of VAs

The suboccipital VA (V3 segment) extends from the C2 transverse foramen to the dura mater of the foramen magnum. The V3 initially courses vertically between the C2 and C1 transverse foramina, then runs horizontally over the C1 groove, and finally obliquely upward before piercing the dura mater. The VAs in the CVJ are divided into 3 parts. The first part corresponds to the course in the foramen of the transverse process of the C1–2 and is called the vertical segment of V3 (V_{3v}). The second part courses in the bony groove of C1 and is called the horizontal segment of V3 (V_{3h}). The third segment, which leaves the groove and travels up the dura mater is called an oblique portion (V_{3o}). One case with the bony ring was found on the C1 in the PB group, and 2 cases were found in the VR group.

The V3 segment has 4 vascular loops. The first loop, known as the inferior medial loop, which directs the artery laterally and

slightly posteriorly, occurs at the transverse foramen of the C2. The next loop, the inferior lateral loop, continues immediately, directing the artery upward and slightly anterior toward the transverse foramen of the C1. The third loop, the superior lateral loop, is located at the point where the V_{3v} segment turns inferiorly into a horizontal position (V_{3h}) in the groove of the posterior arch of the C1. Finally, the fourth loop, the superior medial loop, surrounds the condyle of the C1 and brings the V3 segment to its dural foramen. The distances of the VA and surrounding structures were measured (Table 1).

Measurement of bony structures

The measurement of bony structures in the CVJ includes the occipital condyle, foramen magnum, and foramen of transverse process of the C1. The measurement results are shown in Table 2.

Discussion

The suboccipital segment of the VA is the third part of the VA, which varies significantly because of pathological changes resulting from the local tumor and its own variation features [20]. According to Abd El-Bary et al. [21] the V3 enters the transverse foramen of the C2, where it runs in a vertical, slightly anterior direction. Just above the transverse foramen of the C1, the artery changes direction dorsally and runs further in the sagittal plane. In most cases, this change in direction is associated with an acute angle, but in some cases the change is in a posteromedial direction. The artery then changes its direction again and runs transversely above the posterior arch of the C1, and goes upward by the atlanto-occipital membrane penetrating the dura into the posterior fossa. The course of the VA V3 is divided into 3 portions: a vertical portion between the transverse processes of C2 and C1; a horizontal portion (V_{3h}) in the groove of the posterior arch of the

Table 2. Measurement of bony structures in the CVJ.

GROUP	PB GROUP	VR GROUP
No. of sides	30	40
Dist. bet. medial borders upper rims of the two C1TPF (mm)	54.23±5.86	53.87±5.67
Dist. bet. post. Tb. of atlas & apex of mastoid process (mm)	52.44±4.66	54.27±5.49
Dist. bet. lateral margin of TPA & apex of mastoid process (mm)	22.62±2.32	23.15±2.65
Transverse dia. of FM (mm)	27.28±3.18	28.35±3.41
Long. dis. of FM (mm)	33.76±3.47	35.15±3.81
Long. length of OC (mm)	21.95±2.45	21.27±2.34
Transverse length of OC (mm)	11.80±1.86	11.47±1.74
Dist. bet. post. marg. of OC & post. marg. Of FM (mm)	23.91±3.48	24.25±3.17
Dist. bet. lateral marg. of OC & AMP (mm)	25.47±3.09	25.32±3.14
Dist. bet. marg. of OC & post. marg. of hypoglossal canal (mm)	8.16±1.50	8.43±1.11
Dist. bet. marg. of OC & post. marg. of jugular foramen (mm)	16.16±1.50	17.36±1.73
Transverse dia. of foramen of TPA (mm)	6.46±0.78	6.53±0.72
Long. dia. of foramen of TPA (mm)	6.77±0.79	6.42±0.84

Dist. – distance; bet. – between; dia. – diameter; post. – posterior; Tb. – tubercle; TPA – transverse process of atlas; long. – longitudinal; OC – occipital condyle; FM – FM; AMP – apex of mastoid process; TPF – foramen of transverse process.

atlas; and an oblique portion where it leaves this groove and travels up to the dura mater.

This study focused on the anatomy of the suboccipital segment in the CVJ. In this study, 4 vascular loops of the V3 were found in the 2 groups, as mentioned by Duan [20]. Lang [22] found that the distance between the middle line of the entrance of the VA to the lower rim of the TPF of the atlas was 27.78 mm (22–27). Our measurement yielded 28.64±2.67 mm in the PB group and 29.23±2.89 mm in the VR group. Lang measured the outer diameter of the VA in the middle region of the atlantal part to be 4.20 mm (2.5–6). In our study, the diameters of the VA at the end of the groove and the foramen of the C2 transverse process were 4.02±0.46 mm and 4.25±0.51 mm, respectively, in the PB group and 3.54±0.44 mm and 4.47±0.62 mm, respectively, in the VR group. No significant difference was found between the groups (P>0.05).

The other measurements of distance between the VAs and surrounding structures indicated no significant difference between the 2 groups. These results were similar to those of Lang [22].

Acquiring full and individual information about the anatomy of VAs before surgery in the CVJ is urgently needed. The VAs can be imaged with a variety of techniques. Moniz was credited with the first cerebral angiogram. Since then, various techniques have been developed for imaging the anatomy of the Vas [1,10,20,23]. However, physicians needed to put these images together in the brain before surgery to ascertain relationship

between the VAs and tumors, and virtual reality technology combined these pictures together.

Conclusions

In summary, VR technology can demonstrate the anatomical structures of the vertebral arteries and their bony structures intuitively and individually in 3 dimensions. VR can provide valuable individual anatomical information for resection surgeries on tumors in the CVJ.

Acknowledgements

We gratefully acknowledge the support and valuable contributions of academicians Liang-Fu Zhou M.D, Xiao-Dong Liu Ph.D., M.D, (Shanghai Huashan Hospital), Hua Zhang Ph.D. (Shanghai Jiaotong University), Xiao-Feng Tao, Ph.D. M.D. (Shanghai Changzheng Hospital), and Technician Lin (Anatomy Department of Shanghai Medicine Institute affiliated Fudan University).

Conflict of interest statement

We have no interest with the Dextroscope company and have no other conflict of interest to declare. Anatomical data were obtained by one of authors who works in the Anatomy Department of Shanghai Medicine School affiliated with Fudan University, so there are no legal or ethical issues to declare in this study.

References:

- Govsa F1, Ozer MA, Celik S, Ozmutaf NM: Three-dimensional anatomic landmarks of the foramen magnum for the craniovertebral junction. *J Craniofac Surg*, 2011; 22(3): 1073–76
- Ackerman MJ, Yoo T, Jenkins D: From data to knowledge – the Visible Human Project continues. *Stud Health Technol Inform*, 2001; 84(Pt 2): 887–90
- Deutsch JC: Applications of the Colorado Visible Human Project in gastroenterology. *Clin Anat*, 2006; 19(3): 254–47
- Shi P1, Wang Y, Zhao H et al: [Heart segmentation based on mathematical morphology And Otsu in visible human project images]. *Sheng Wu Yi Xue Gong Cheng Xue Za Zhi*, 2007; 24(5): 996–1000
- Stern M: Dystopian anxieties versus utopian ideals: medicine from Frankenstein to The Visible Human Project and Body Worlds. *Sci Cult (Lond)*, 2006; 15(1): 61–84
- Yang de L1, Xu QW, Che XM et al: Clinical evaluation and follow-up outcome of presurgical plan by Dextroscope: a prospective controlled study in patients with skull base tumors. *Surg Neurol*, 2009; 72(6): 682–89; discussion 689
- Kockro RA1, Serra L, Tseng-Tsai Y et al: Planning and simulation of neurosurgery in a virtual reality environment. *Neurosurgery*, 2000; 46(1): 118–35; discussion 135–37
- Tubbs RS1, Shah NA, Sullivan BP et al: Surgical anatomy and quantitation of the branches of the V2 and V3 segments of the vertebral artery. Laboratory investigation. *J Neurosurg Spine*, 2009; 11(1): 84–87
- Thiel HW: Gross morphology and pathoanatomy of the vertebral arteries. *J Manipulative Physiol Ther*, 1991; 14(2): 133–41
- Tay KY1, U-King-Im JM, Trivedi RA et al: Imaging the vertebral artery. *Eur Radiol*, 2005; 15(7): 1329–43
- Sylla S: [The cervicothoracic ganglion and segments V1, V2 and V3 of the vertebral artery]. *Dakar Med*, 1979; 24(4): 328–40
- Rickenbacher J: [The Suboccipital and Intracranial Segment of the Vertebral Artery]. *Z Anat Entwicklungsgesch*, 1964; 124: 171–78
- Muralimohan S, Pande A, Vasudevan MC, Ramamurthi R: Suboccipital segment of the vertebral artery: a cadaveric study. *Neurol India*, 2009; 57(4): 447–52
- Kiresi D1, Gumus S, Cengiz SL, Cicekcibasi A: The morphometric analysis of the V2 and V3 segments of the vertebral artery: normal values on MDCT. *Comput Med Imaging Graph*, 2009; 33(5): 399–407
- Gupta T: Quantitative anatomy of vertebral artery groove on the posterior arch of atlas in relation to spinal surgical procedures. *Surg Radiol Anat*, 2008; 30(3): 239–42
- George B: Extracranial vertebral artery anatomy and surgery. *Adv Tech Stand Neurosurg*, 2002; 27: 179–216
- Castillo C1, Viñas FC, Gutikhonda M, Diaz FG: Microsurgical anatomy of the suboccipital segment of the vertebral artery. *Neurol Res*, 1998; 20(3): 201–8
- Bruneau M, Cornélius JF, George B: Anterolateral approach to the V2 segment of the vertebral artery. *Neurosurgery*, 2005; 57(4 Suppl.): 262–67; discussion 262–67
- Akar ZC1, Dujovny M, Slavin KV et al: Microsurgical anatomy of the intracranial part of the vertebral artery. *Neurol Res*, 1994; 16(3): 171–80
- Duan S, Lv S, Ye F, Lin Q: Imaging anatomy and variation of vertebral artery and bone structure at craniocervical junction. *Euro Spine J*, 2009; 18(8): 1102–8
- Abd el-Bary TH, Dujovny M, Ausman JI: Microsurgical anatomy of the atlantal part of the vertebral artery. *Surg Neurol*, 1995; 44(4): 392–400; discussion 400–1
- Lang J, Kessler B: About the subclinical part of the vertebral artery and the neighboring bone-joint and nerve relationships. *Skull Base Surge*, 1991; 1(1): 64–72
- Lévy C, Laissy JP, Raveau V et al: Carotid and vertebral artery dissections: three-dimensional time-of-flight MR angiography and MR imaging versus conventional angiography. *Radiology*, 1994; 190(1): 97–103